ELSEVIER

PII: S0032-3861(96)01076-2

Polymer Vol. 38 No. 18, pp. 4697–4703, 1997

0032-3861/97/$17.00+0.00

Phase diagrams calculated for sheared ternary polymer blends

R. Horst and B. A. Wolf*

Institut für Physikalische Chemie, Johannes Gutenberg-Universität, Jakob-Welder-Weg 13, D-55099 Mainz, Germany

(Received 8 August 1996; revised 14 October 1996)

On the basis of the generalized Gibbs energy of mixing $G_{\dot{\gamma}}$ (which is the sum of the Gibbs energy for zero shear and the energy the system stores in steady flow) phase diagrams were calculated as a function of shear rate $\dot{\gamma}$ for ternary model blends. This modelling uses simple equations for the description of the stagnant systems (Flory–Huggins) and for the contributions resulting from flow. Surface and alignment effects are neglected. A new procedure, which does not require the derivatives of $G_{\dot{\gamma}}$ with respect to composition, was used to that end. Choosing typical values for the binary interaction parameters and molar masses, four classes of ternary systems were studied in greater detail. Under equilibrium conditions, with two of them there only exist one-phase and two-phase regions in the temperature range of interest. At least one three-phase domain occurs with the other two types of ternary mixtures. In addition to all effects observed for binary systems, the following new phenomena were calculated: (i) twofold disappearance of closed loops of immiscibility and twofold reappearance; (ii) creation and annihilation of three phase areas; and (iii) creation and annihilation of islands of homogeneity in the centre of the ternary phase diagram. © 1997 Elsevier Science Ltd.

(Keywords: shear; polymer blends; miscibility)

INTRODUCTION

The influence of flow on the phase behaviour of polymer blends has been a topic of research for many years[1–10]. It is also of great technical interest, the most prominent example being the extrusion process. Theoretical considerations of the authors have so far dealt with strictly binary blends[11]. The outcome of these calculations are in very good qualitative agreement[12] with related experimental results. In view of the fact that polymers in technical applications nearly always contain additives and normally exhibit broad molar mass distributions, we extended our theoretical approach—which is again based on a generalization of the Gibbs energy of mixing—to ternary polymer blends.

THEORETICAL BACKGROUND

The generalized Gibbs energy of a flowing system, $G_{\dot{\gamma}}$, differs from G_z, that of the corresponding stagnant one. Calling the difference $E_{\dot{\gamma}}$, one can write

$$G_{\dot{\gamma}} = G_z + E_{\dot{\gamma}} \tag{1}$$

If $E_{\dot{\gamma}}$ is sufficiently small compared with G_z, the ordinary tools of thermodynamics can be applied to $G_{\dot{\gamma}}$.

G_z contains the entire information required for the description of systems at rest. All contributions due to flow fields are incorporated into $E_{\dot{\gamma}}$; the most important of them are:

(a) deformation of molecules (as manifested in rheology, e.g. changes in the number of entanglements);
(b) orientation of molecules or of parts of them;
(c) orientation at larger length scales;
(d) interfacial effects;
(e) changes in the contact statistics of segments.

In order to perform model calculations on the basis of the above relation, theoretical expressions for the two constituents of $G_{\dot{\gamma}}$ are required. Since it is the aim of the present paper to study in a qualitative manner which flow induced changes in the phase behaviour of blends one can expect, the equations are chosen as simple as possible. This implies a minimization of the numbers of parameters and keeps the modelling manageable. Naturally, these simplifications limit the results to qualitative statements, it appears unlikely that real systems can be described in a quantitative manner by such simple equations.

For G_z it is—as usual—assumed that the Flory–Huggins relation suffices for the modelling of the thermodynamics of the stagnant systems. In the case of $E_{\dot{\gamma}}$ we assume that changes in the contact statistics (e) are negligible. Interfacial phenomena (d) are expected to become particularly important with highly disperse systems (e.g. formation of 'string phases'[13]); they should, however, be negligible as long as one does not transpass the limits of homogeneity. Orientation at larger lengths scales (c)—like the alignment of microstructures in systems containing block copolymers[14]—are presently also ruled out. Orientations of macromolecules (b) should become dominant for highly dilute polymer solutions[15], whereas they appear of minor importance here. For the polymer blends of present interest, molecular deformations (a) are postulated to be the decisive contribution to $E_{\dot{\gamma}}$.

* To whom correspondence should be addressed

For this reason the term $E_{\dot{\gamma}}$ was already in the past approximated by the stored energy E_s[16] (the energy the system takes up during the attainment of steady flow) and equation (1) can be rewritten as

$$G_{\dot{\gamma}} = G_z + E_s \tag{2}$$

The above procedure has so far proven to be very suitable in the qualitative description of experimental observation of shear induced changes in the phase separation behaviour of polymer solutions[17] and of polymer blends[12].

Gibbs energy of mixing of the stagnant system

The Gibbs energy of mixing for zero shear conditions G_z is accessible via the Flory–Huggins equation

$$\frac{\overline{\overline{\Delta G_z}}}{RT} = \sum_{i=1}^{K} \frac{1}{N_i} \varphi_i \ln \varphi_i + \sum_{i=1}^{K-1} \sum_{j=i+1}^{K} g_{ij} \varphi_i \varphi_j \tag{3}$$

where φ_i is the volume fraction of component i, K is the number of components (for the actual ternary systems $K = 3$), and g_{ij} is the interaction parameter between components i and j.

N_i the number of segments per molecule of component i, is calculated by dividing the molar volume V_i by V_s, the molar volume of the segment.

Stored energy

In mixtures containing polymers considerable amounts of energy can be stored as compared with mixtures of low molar mass components. In the melt the chains between entanglement points are stretched as the liquid flows and energy can be regained upon the relaxation of chains into their equilibrium dimensions after the cessation of shear. Since—at constant composition and shear rate $\dot{\gamma}$—the number of entanglements per chain increases with molar mass, the stored energy E_s also becomes larger as long as the shear rates are chosen sufficiently low so that one does not leave the region of Newtonian flow behaviour; within this range, E_s is proportional to $\dot{\gamma}^2$. As the shear rates exceed the inverse of the characteristic viscometric relaxation time, however, disentanglement processes start and the number of entanglements decreases[18]. This fact implies that the stored energy may diminish as $\dot{\gamma}$ is raised to high enough shear rates.

The relations used to calculate the stored energy E_s have been given in ref. 11. Here only the indispensable ones are briefly recalled.

$$\overline{\overline{E_s}} = V_s \langle J_e^0 \rangle (\langle \eta \rangle \dot{\gamma})^2 |\langle \eta \rangle \dot{\gamma}|^{-2d^*} \tag{4}$$

where $d^* = -(\partial \ln \eta / \partial \ln \dot{\gamma})$, V_s is the molar volume of the segment, J_e^0 is the steady state shear compliance, η is the viscosity, $\dot{\gamma}$ is the shear rate, and $\langle\ \rangle$ mark quantities of the mixture.

The shear rate dependence of η is accessible by means of Graessley's equation[18]. The longest viscometric relaxation time τ_0, contained in this relation, is often[11] replaced by the Rouse relaxation time[19]. The steady state shear compliances of the pure components (indicated by the index i) are related to τ_0 and the zero-shear viscosity η_0 by

$$J_{ei}^0 = \frac{\tau_{0i}}{\eta_{0i}} \tag{5}$$

The mixing rules for η_0 and J_e^0 from ref. 20 can be extended for ternary systems in the following manner

$$\langle \eta_0 \rangle^{1/3.4} = \sum_i w_i \eta_{0i}^{1/3.4} \tag{6}$$

$$\langle J_e^0 \rangle = \frac{\sum_i w_i \eta_{0i}^{4.4/3.4} J_{ei}^0}{\langle \eta_0 \rangle^{4.4/3.4}} \tag{7}$$

The expressions are based on the exponential relation between η_0 and the molar mass M

$$\eta_0 = K_M M^{3.4} \tag{8}$$

The temperature dependence of η_0 can be represented by the Arrhenius equation, as long as one is not too close to the glass transition of the polymer

$$\eta_0 = \eta_0^{T_c} \exp\left[\frac{E^{\neq}}{RT}\left(\frac{1}{T} - \frac{1}{T_c}\right)\right] \tag{9}$$

$E^{\neq}$ represents the activation energy of viscous flow and T_c, the critical temperature, is chosen as the reference temperature for the present purposes.

Calculation procedure

In view of the fact that it often turns out very difficult or even impossible to express E_s as a function of composition in a closed analytical form, the standard thermodynamic procedure is left. Instead of calculating the first derivatives of the Gibbs energy of mixing yielding binodal lines (equality of the chemical potentials of the components in the coexisting phases) and the second derivatives, required for the calculation of spinodal lines, the present approach utilizes the thermodynamic criterion for equilibrium in a direct manner. It is exclusively based on the reduction of the (generalized) Gibbs energy associated with spontaneous processes in closed systems. A detailed discussion of the applied calculation method is given in ref. 21. For the computation of the entire phase diagram it turns out expedient to start with the calculation of the spinodal line.

Spinodal lines. To separate the unstable from the metastable plus stable region of a *binary system*, the concentration axis (in the actual case the volume fraction φ of one component) is divided into n sections. At a given overall composition φ^{oa} the distance from one point to the next—which defines the accuracy with which the spinodal condition can be determined—is therefore $1/n$. The stability of a *homogeneous* mixture (information referring to that state is marked by the superscript hom) is then examined by comparing ΔG^{hom} with ΔG^{dem}, the Gibbs energy of mixing into a hypothetical state for which two phases coexist that differ in composition from φ^{oa} only marginally [namely by $\pm 1/(2n)$]. In case ΔG^{dem} is less than ΔG^{hom} the system is unstable, else it is either metastable or stable.

For the *ternary systems* of present interest the procedure is somewhat more complicated. In this case the scanning pattern inside the ternary diagram consists of $(n-2)(n-1)/2$ points (for given φ_1 the second variable can only assume values between 0 and $1 - \varphi_1$). The binary sub-systems need not be treated separately, as long as n is chosen sufficiently large; under these

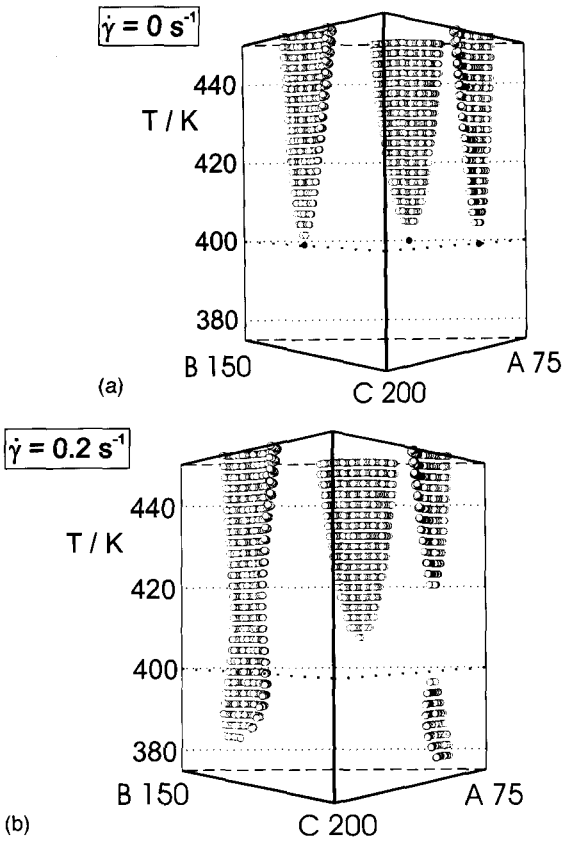

Figure 1 Spinodal conditions for the ternary model blend A 75/B 150/C 200 (the numbers give the molar masses in kg mol^{-1}) in the temperature interval from 380 to 450 K (a) at zero-shear conditions and (b) for the given shear rate. The full circles of (a) indicate the critical points. The binary interaction parameters are fixed by the condition $T_c = 400$ K and equation (15)

conditions the number of mixtures for which calculations have to be performed equals approximately $n^2/2$.

In order to check the thermodynamic stability of a certain mixture by analogy to the procedure outlined above for binary systems, it is necessary to vary the direction of the secant in the ternary diagram. Marking the two phases of slightly different composition by the superscripts (1) and (2), respectively, and introducing $\phi^{(1)}$ for the fraction of the total volume that is occupied by phase 1, the following relation expresses the mass balance for a system of K components:

$$\varphi_i^{oa} = \phi^{(1)}\varphi_i^{(1)} + (1-\phi^{(1)})\varphi_i^{(2)}, \quad i = 1, \ldots, K \qquad (10)$$

In order to discover whether a certain mixture is represented by a point inside the spinodal area of the ternary diagram, the secant of length $1/n$ must be found for which ΔG^{dem} is minimum; if this value is less than ΔG^{hom}, the system is unstable. In order to find this minimum, the secant is rotated around the given overall composition. The φ_i values of the different two phase situations are fixed by *adding* the following increments to φ_i^{oa} in the case of *phase 1* and *subtracting* them in the case of *phase 2*

$$\Delta\varphi_1 = -\sin\left(\frac{\pi}{3}+\alpha\right)\frac{0.5}{n} \qquad (11)$$

$$\Delta\varphi_2 = \sin(\alpha)\frac{0.5}{n} \qquad (12)$$

$$\Delta\varphi_3 = \sin\left(\frac{\pi}{3}-\alpha\right)\frac{0.5}{n} \qquad (13)$$

α, the angle between the line for constant φ_2 and the secant, can assume values between 0 and π, since a rotation of $\alpha + \pi$ is identical with a rotation of α and an exchange of the two phases. The value of α for which ΔG^{dem} reaches its minimum has to be determined by an iteration process.

The calculation uses $\overline{\overline{\Delta G}}$, the Gibbs energy of mixing for one mol of *segments*, the size of which is defined by V_s, the molar volume of the segments. Connecting the ΔG^{hom} values of the two phases of the demixed system, i.e. constructing a secant to $\Delta G(\varphi)$, and reading the value of this secant at the overall composition yields ΔG^{dem} according to:

$$\overline{\overline{\Delta G^{dem}}} = \phi^{(1)}\overline{\overline{\Delta G^{hom(1)}}} + (1-\phi^{(1)})\overline{\overline{\Delta G^{hom(2)}}} \qquad (14)$$

If ΔG^{dem} is less than ΔG^{hom} for at least one α value, the overall composition lies within the unstable area, since the system cannot resist fluctuations in concentration (no energy barrier for phase separation). In the opposite case the mixture is stable, or at least metastable (energy barrier for demixing). Checking all points inside the phase diagram yields the entire unstable area, and thus the spinodal line as its boundary, which can be easily visualized by deleting all points of instability that are totally surrounded by neighbours which also lie within the spinodal region.

The current calculations were typically performed for $n = 200$ on an IBM RISC 6000 computer by means of a program written in Pascal. The representative time required to obtain the spinodal for a flowing ternary polymer blend amounts to 2 h.

Tie lines. The first step of the calculation consists in the selection of the overall composition of the system (φ_1^{oa} and φ_3^{oa}). In order to guarantee that a tie line exists, it is checked that the chosen point lies within the unstable area of the phase diagram. For a ternary system and known φ_i^{oa} the tie lines are fully described by three parameters. In the present case these three parameters are two volume fractions of phase 1 ($\varphi_1^{(1)}$ and $\varphi_3^{(1)}$) and the fragment of the total volume that is occupied by phase 1 ($\varphi^{(1)}$). The composition of phase 2 can then be calculated according to equation (10).

By means of a Simplex fit, that can be performed on an ordinary personal computer within a few seconds, it is tested for a given overall composition which values of the three parameters $\varphi_1^{(1)}$, $\varphi_3^{(1)}$, and $\phi^{(1)}$ yield the largest reduction in the Gibbs energy upon demixing (minimum in ΔG^{dem}). This procedure is analogous to the one used in the calculation of spinodals, except for the fact that the length of the line connecting two points on the surface $\Delta G^{hom}(\varphi_1, \varphi_3)$ is no longer given by $1/n$ but treated as a variable. As can be easily visualized, the secant that fulfils the above minimum condition is identical to the tie line and part of the tangential plane to $\Delta G^{hom}(\varphi_1, \varphi_3)$ which fulfils the condition that the chemical potentials of the components are identical in the coexisting phases. The desired binodal line is obtained by computing a sufficient number of tie lines for different overall compositions and connecting their endpoints.

RESULTS

In the assessment of the results presented in the following, one has to keep in mind that interface and

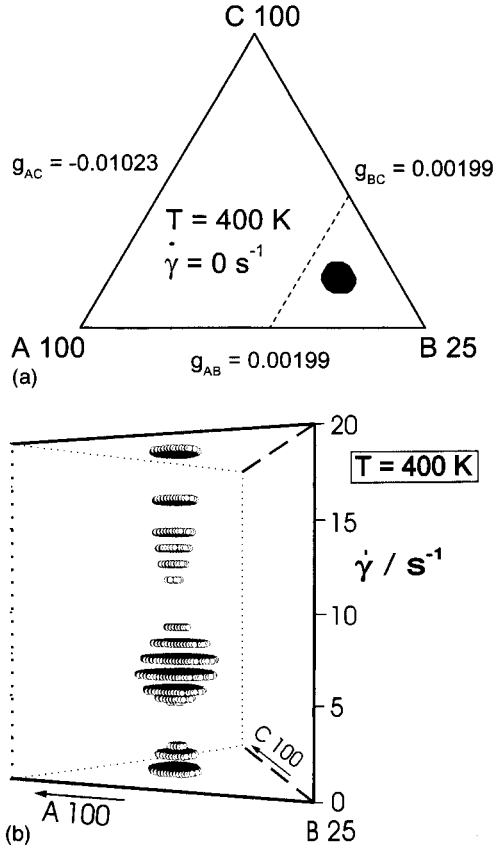

Figure 2 Phase diagrams of the model blend A 100/B 25/C 100 (the numbers give the molar mass in kg mol^{-1}) at 400 K. (a) shows the island of immiscibility (unstable area) under equilibrium conditions; the binary interaction parameters are indicated at the edges of the ternary diagram. The variation of the extent of the unstable area with shear rate is given in (b) for the interval from 0 to 20 s^{-1}; the part of the diagram which is shown in (b) is indicated in (a) by the broken line

alignment effects were not incorporated in the modelling. This means that phenomena caused by these effects are not covered by the present approach. The values of the parameters used in the following calculations are 10^{-4} m^3 mol^{-1} for V_s, 1000 kg m^{-3} for the density of the polymers (required for the evaluation of the molar volumes from the molar masses), 400 K for T_g, 10^{-3} Pa s for K_M [equation (8)] and 30 kJ mol^{-1} for $E^{\neq}$ [equation (9)]. Parameters differing from these values are indicated in the graphs.

In the first ternary example shown in *Figure 1* the subsystems consist of the binary systems of the preceding paper[22] on binary blends. All three molar masses are different. For the temperature dependence of the three binary interaction parameters the following relation is selected

$$g_{ij} = g_{ijc} + 3 \times 10^{-6}(T - T_c) \qquad (15)$$

where

$$g_{ijc} = 0.5\left(\frac{1}{\sqrt{N_i}} + \frac{1}{\sqrt{N_j}}\right)^2$$

and is the critical interaction parameter for the binary subsystem consisting of components i and j.

Figure 1a shows the spinodal conditions for the stagnant blend. The pure component C 200 is shown in the foreground, A 75 and B 150 are situated in the background. Since the critical composition is always situated closer to the lower molar mass component, the largest homogeneous area is located in the corner of C 200, which is the component with the highest molar mass. The critical temperature of all binary subsystems is fixed at 400 K. The interaction parameters resulting from that assumption and from the value of 3×10^{-6} chosen for the proportionality constant of equation (15) remain so low within the temperature range of interest, that the three miscibility gaps do not coalesce.

The application of a shear rate of 0.2 s^{-1} changes the phase diagrams of the three subsystems in a very different way. The subsystem with the lowest molar mass components A 75/B 150 shows shear induced mixing only, i.e. the homogeneous area expands as the system flows. The reason is that the characteristic viscometric relaxation times of the mixtures remain relatively small, and the viscosity shows Newtonian behaviour. Therefore the stored energy increases monotonously with the content of B and the miscibility is enhanced.

For the second subsystem A 75/C 200 the effect of shear induced mixing is more pronounced than for the first. The minimum of the main miscibility gap of the sheared blend assumes the highest values of the three subsystems. But simultaneously a closed miscibility gap is created at 380 K to 395 K. Here the relaxation times are so long that the flow behaviour becomes non-Newtonian at the lower temperatures of *Figure 1* and one additionally observes shear induced demixing (the flowing blend is two phase where the stagnant blend is homogeneous).

For B 150/C 200 the relaxation times are so long even at the higher temperatures that shear induced demixing is observed at all temperatures around T_c. At 0.2 s^{-1} the island of immiscibility has already merged with the main miscibility gap. All phenomena resulting for the present ternary system are identical with that already calculated for binary blends, i.e. no new shear-induced phenomena show up.

The second ternary blend (*Figure 2*) is symmetrical in the sense that the molar masses of A and C are equal, and so are the interaction parameters of these two components with B. In case of sufficiently large negative values of g_{AC} and suitable g_{AB} and g_{BC}, the stagnant blend exhibits a closed miscibility gap.

Figure 2a shows the entire phase diagram (in terms of the spinodal area), whereas *Figure 2b* only presents the corner close to the pure component B. Equilibrium diagrams like this have been observed for a ternary mixture of polystyrene, poly(2-chlorostyrene) and polycyclohexylacrylate[23]. According to the present calculations the phase behaviour of such types of blends should be very pronouncedly influenced by shear. At small $\dot{\gamma}$, the miscibility gap shrinks until the shear induced mixing is so strong that the components become completely miscible. At somewhat higher $\dot{\gamma}$ values the gap emerges again and grows much larger than the equilibrium unstable area. Increasing $\dot{\gamma}$ still further leads to a second range of shear induced mixing. Where the interaction parameters are chosen properly, as in the present case, the island of immiscibility disappears a second time. Finally, at still higher shear rates the gap emerges again and approaches the shape of the unstable area of the stagnant blend again. The succession of shear effects is in perfect agreement with the results for binary blends[11].

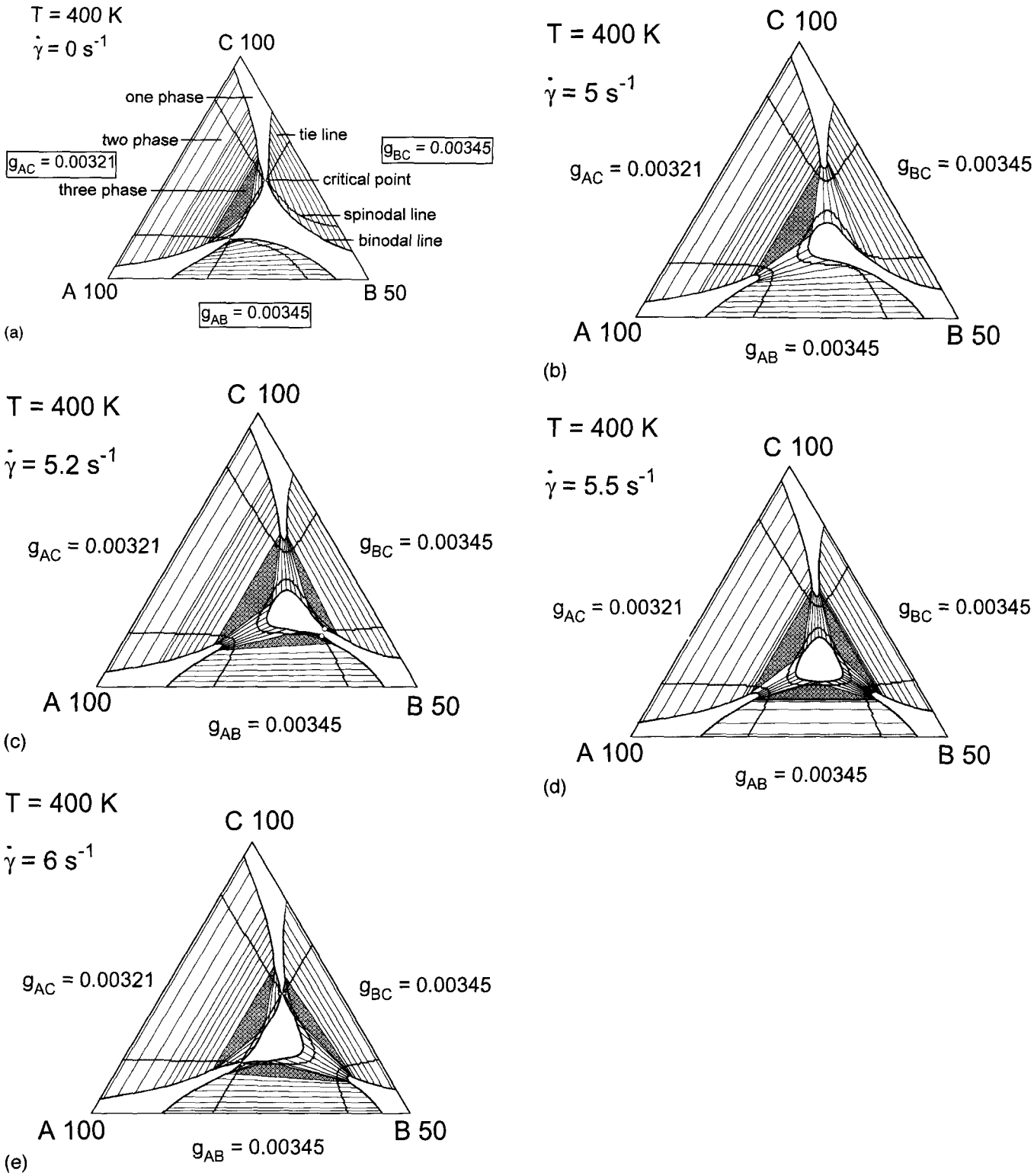

Figure 3 Phase diagram of the model blend A 100/B 50/C 100 at 400 K and the given shear rates. The tie lines, spinodal line and the critical points are also given. The three phase areas are indicated by shading

We now turn to mixtures which are again symmetrical—like the previous one—the molar mass of B is, however, doubled and the value of the interaction parameters of components A and C with B is raised; furthermore, A and C are no longer compatible, i.e. all constituents of the ternary system exhibit a much lower mixing tendency. *Figure 3* shows an example of the entire phase diagram (including tie-lines and binodals) calculated for such blends; parameters are chosen so that the three miscibility gaps in the equilibrium situation are just big enough to leave areas of homogeneity between them.

From *Figure 3a* it can be seen that four critical points and a three phase area—located inside the A–C miscibility gap—are calculated for the stagnant ternary blend. The effects of shear are shown in *Figure 3b* to *Figure 3e*, this time—as with the next example—not dealing with low shear rates where shear-induced mixing occurs, since no new phenomena result. In *Figure 3b*

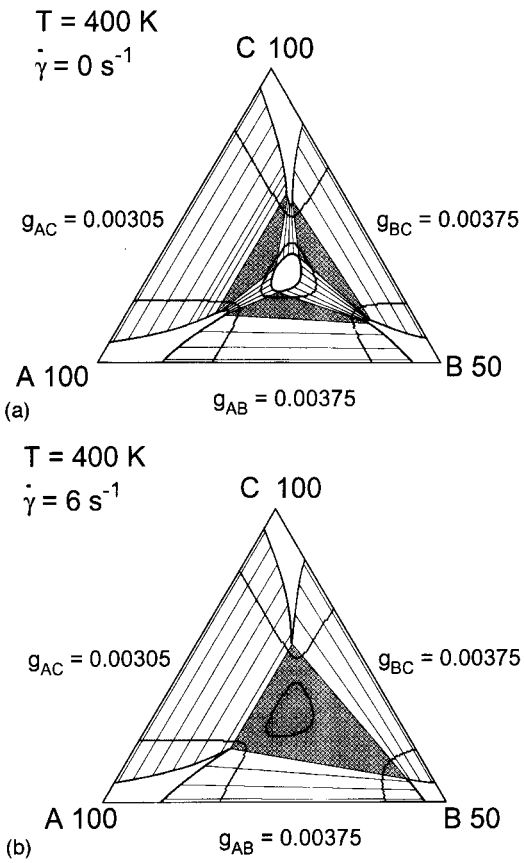

Figure 4 Spinodal and tie lines in the phase diagram for the modal blend A 100/B 50/C 100 at 400 K for zero shear (a) and at 6 s^{-1} (b)

($\dot{\gamma} = 5\,s^{-1}$) the influence of shear is most prominent on the side of the higher molar mass components of the ternary diagram. Therefore the unstable area is particularly increased where the unstable area of A/C comes close to the two other miscibility gaps. This means the spinodal areas of the three subsystems coalesce in this area so that the critical points disappear and one large unstable area is created.

With increasing $\dot{\gamma}$ the area of shear induced demixing shifts towards the lower molar mass component B as can be seen in *Figure 3c*; this finding is in accord with the results of calculations for binary polymer blends[11]. The enhancement of incompatibility is so strong that two new three phase areas are created and—associated therewith—two new critical points.

Upon a further augmentation of $\dot{\gamma}$ (cf. *Figure 3d*) the unstable areas coalesce at all three regions in which the three equilibrium miscibility gaps come close together. So again one large two-phase area is created which now, however, surrounds an island of stability. All critical points have disappeared and flowing blends with compositions located in the stable area in the centre of the ternary diagram become homogeneous when sheared at the given rate.

The effects resulting from still higher $\dot{\gamma}$ values are shown in *Figure 3e*. In this case the region of shear induced demixing has shifted so far towards the component B that only the unstable areas A/B and B/C coalesce, whereas that at A/C remains apart. So the flowing blend exhibits two unstable areas with 3 three phase areas and 4 critical points.

The sequence of phase diagrams presented in *Figures 3b–e* demonstrate some new phenomena, which cannot be observed with binary blends, due to the absence of three phase areas. One is the creation of three phase areas, another the production of a homogeneous region within a demixed area by shear.

In the next example the opposite observation is discussed, namely the disappearance of an island of homogeneity and of three-phase areas resulting from the application of shear. For these calculations the component of the ternary blend and the symmetry are chosen identical with the previous example. However, AB and BC are postulated to be somewhat less and AC somewhat more compatible. *Figure 4* shows the phase diagrams obtained under these conditions for the stagnant and for the flowing system.

Even in the stagnant blend there is only one large unstable area. The equilibrium situation for the actual blend is very similar to that of the flowing blend of *Figure 3d*: a stable island in the centre, 3 three phase areas and 6 two phase areas. *Figure 4b* demonstrates the effect of a shear rate of 6 s^{-1}: the unstable area increases, the metastable island is reduced, but still exists, whereas the stable island vanishes. A large three phase area is formed covering the region of the island and the 3 equilibrium three phase areas. The effects of shear are in the actual example just opposite to the previous one, since the number of three phase areas decreases and an island of homogeneity disappears in the flowing polymer blend.

OUTLOOK

The extension of the theoretical approach starting from a generalized Gibbs energy to ternary polymer blends has produced a multitude of new effects. These numerical computations were performed according to a new method—which does not require fitting functions for the stored energy—and consequently does not suffer from any inadequacies resulting from imprecise fitting functions. The calculation of the phase diagrams of ternary polymer blends constitutes the basis for an extension of the present computations to polymer blends containing additives, e.g. blends of two homopolymers A and B and a copolymer A–B, or even C–D. The effect of polydispersity can also be modelled by mixing a homopolymer A with two samples of homopolymer B differing in molar mass.

ACKNOWLEDGEMENTS

The authors wish to thank the European Union (Brite/EuRam II) and the Deutsche Forschungsgemeinschaft (DFG) for the support of this work and Cora Krause for critical reading of the typescript.

REFERENCES

1. Mazich, K. A. and Carr, S. H., *J. Appl. Phys.*, 1983, **54**, 5511.
2. Tirrell, M., *Fluid Phase Equilibria*, 1986, **30**, 367.
3. Lyngaae-Jørgensen, J. and Søndergaard, K., *Polym. Eng. Sci.*, 1987, **27**, 351.
4. Katsaros, J. D., Malone, M. F. and Winter, H. H., *Polym. Eng. Sci.*, 1989, **29**, 1434.
5. Nakatani, A. I., Kim, H., Takahashi, Y., Matsushita, Y., Takano, A., Bauer, B. J. and Han, C. C., *J. Chem. Phys.*, 1990, **93**, 795.

6. Kammer, H. W., Kummerloewe, C., Kressler, J. and Melior, J. P., *Polymer*, 1991, **32,** 1488.
7. Hindawi, I. A., Higgins, J. S. and Weiss, R. A., *Polymer*, 1992, **33,** 2522.
8. Larson, R. G., *Rheol. Acta,* 1992, **31,** 497.
9. Muniz, E. C., Nunes, S. P. and Wolf, B. A., *Macromol. Chem. Physics* 1994, **195,** 1257.
10. Onuki, A., *J. Non-Cryst. Solids*, 1994, **172,** 1151.
11. Horst, R. and Wolf, B. A., *Rheol. Acta,* 1994, **33,** 99.
12. Higgins, J. S., Fernandez, M. L., Horst, R. and Wolf, B. A., *Polymer*, 1995, **36,** 149.
13. Hashimoto, T., Matsuzaka, K., Moses, E. and Onuki, A., *Phys. Rev. Lett.*, 1995, **74,** 126
14. Jackson, C. L., Barnes, K. A., Morrison, F. A., Mays, J. W., Nakatani, A. I. and Han, C. C., *Macromolecules*, 1995, **28,** 713.
15. Zisenis, M. and Springer, J., *Polymer*, 1994, **35,** 3156.
16. Wolf, B. A., *Macromolecules*, 1984, **17,** 615.
17. Krämer-Lucas, H., Schenck, H. and Wolf, B. A., *Makromol. Chem.*, 1988, **189,** 1613 and 1627.
18. Graessley, W. W., *Adv. Polym. Sci.*, 1974, **16,** 1.
19. Rouse, P. E., *J. Chem. Phys.*, 1953, **21,** 1272.
20. Schuch, H., *Rheol. Acta*, 1988, **27,** 384.
21. Horst, R. *Macromol. Theory Simul.*, 1995, **4,** 449.
22. Horst, R. and Wolf, B. A., *Macromolecules*, 1993, **26,** 5676.
23. Rabeony, M., Siano, D. B., Pfeiffer, D. G., Siakali-Kioulafa, E. and Hadjichristidis, N., *Polymer*, 1994, **35,** 1033.